Bol. Soc. Paran. Mat.
©SPM – E-ISSN-2175-1188
SPM: www.spm.uem.br/bspm

(3s.) **v. 2025 (43) 3** : 1–25.
ISSN-0037-8712
doi:10.5269/bspm.78062

Numerical Analysis of Thermoelastic Wave Behavior in a Micropolar Medium with Dual-Phase-Lag, Nonlocality, and Pre-Stress under Gravitational Influence

Sonia Bajaj* and A. K. Shrivastav

ABSTRACT: This study investigates the transient wave propagation in a micropolar thermoelastic half-space under the influence of gravity, initial stress, and nonlocal effects, within the framework of two-temperature generalized thermoelasticity incorporating the dual-phase lag (DPL) model. The governing equations are formulated considering a quiescent medium subjected to an inclined mechanical load and a gravitational field. An analytical solution is derived using normal-mode analysis to obtain exact expressions for the thermomechanical field variables. Numerical simulations are performed for a magnesium crystal-like material to evaluate the distributions of displacement, stress, and temperature. The results are presented graphically to illustrate the influences of initial stress, non-locality, the two-temperature parameter, and the angle of loading inclination. Comparative analyses are also conducted to highlight the role of these factors on wave behavior, with particular cases discussed as subsets of the generalized model.

Key Words: Nonlocal, micropolar, initial stress, gravity, two-temperature theory, normal mode analysis technique, dual-phase lag.

Contents

1. Introduction

The classical thermoelasticity theory predicts infinite speed for thermal signal propagation, which is physically unrealistic. To address this, Lord and Shulman (1967) introduced a generalized theory with a single thermal relaxation time (LS theory) [1]. Subsequently, Green and Lindsay (1972) proposed a model with two relaxation times (GL theory) [2], both allowing finite thermal wave speeds. Later, Green and Naghdi (1991–1993) developed an alternative framework, the GN theory, divided into three types: GN-I aligns with Fourier's law (no thermal relaxation), GN-II assumes zero entropy production (no dissipation), and GN-III accommodates both types with general dissipation [3]. The classical Fourier law of heat conduction $\mathbf{q}(\mathbf{r},t) = -k\nabla T(\mathbf{r},t)$ predicts an unphysical infinite speed of thermal signal propagation. To address this, Tzou [4] introduced the DPL model, modifying Fourier's law to $\mathbf{q}(P,t+\tau_q) = -k\nabla T(P,t+\tau_T)$, where τ_T and τ_q represent the phase lags of temperature gradient and heat flux, respectively. If both lags vanish, the classical Fourier law is recovered. Recent peer-reviewed studies [5,6,7,8,9,10] have demonstrated the efficacy of the DPL model in validating thermoelastic predictions.

* Corresponding author.

Submitted July 24, 2025. Published October 02, 2025
2010 *Mathematics Subject Classification:* 74A15, 74B10, 74H45, 74J05.

Chen and Gurtin [11,12] introduced a heat conduction model for deformable bodies incorporating two distinct temperatures: the conductive temperature ϕ and the thermodynamic temperature Θ. While ϕ is attributed to heat conduction, Θ is linked to mechanical deformation. Under specific equilibrium conditions, these temperatures may coincide [13], but they generally differ in dynamic situations. A defining feature of this theory is the temperature discrepancy parameter a; when $a = 0$, $\phi = \Theta$, reducing the model to classical thermoelasticity. Youssef [14] formulated the generalized two-temperature thermoelasticity theory, establishing uniqueness results, while Youssef and Al-Lehaibi [15] applied the state-space method to a one-dimensional problem. Further developments include the work of Ezzat and Awad [16] on a two-temperature model along with micropolar thermoelasticity and El-Karamany and Ezzat [17], who presented variational principles and reciprocal theorems for anisotropic Green–Naghdi models. Youssef [18] extended the theory using fractional calculus and moving heat sources. A three-dimensional model with Laplace–Fourier methods was proposed by Ezzat and Youssef [19]. For further refinement, Zhang et al. [20] and Liu et al. [21] introduced advanced modeling approaches in generalized thermoelasticity, incorporating multi-temperature and nonlocal effects.

In classical elasticity theory, gravitational effects are often disregarded due to their relatively small influence in many applications. However, Bromwich [22] was the first to examine the role of gravity in wave propagation within elastic solids, notably in the context of an elastic sphere. Love [23] later demonstrated that the presence of gravity significantly increases Rayleigh wave velocity, particularly at long wavelengths. Biot [24] further analyzed gravitational influences on Rayleigh waves in an incompressible isotropic elastic medium. Recent studies have incorporated these effects into thermoelastic frameworks. For instance, Ailawalia et al. [25] explored the deformation of a rotating two-temperature generalized thermoelastic medium under gravity and different source configurations. Othman and Hilal [26] analyzed the behavior of a rotating thermoelastic material with voids under gravitational forces, while their subsequent work [27] considered the combined impact of gravity and magnetic fields on plane wave propagation in a thermoelastic medium heated by a laser pulse. More recently, Liu et al. [28] and Zhang and Wang [29] extended the analysis to nonlocal and fractional-order thermoelastic models, capturing the complex interplay of gravity, heat, and wave motion in advanced materials.

Micropolar elastic solids are conceptualized as materials composed of particles resembling dumbbell-shaped molecules capable of both translational and rotational motion. Unlike classical elasticity, where deformation is described solely by displacement fields, the micropolar theory incorporates microrotations, leading to the presence of couple stresses in addition to conventional force stresses. As a result, the mechanical response is governed by six degrees of freedom: three for linear displacements and three for microrotations. A comprehensive development of the micropolar elasticity framework, including its kinematic assumptions and constitutive equations, can be found in the monograph by Eringen [30]. The micropolar theory of elasticity has been significantly extended to incorporate thermal effects. Early advancements were made by Nowacki [31,32,33] and later by Eringen [34], who introduced thermomechanical coupling into the micropolar framework. Tauchert et al. [35] derived the fundamental equations for linear micropolar thermoelasticity. Further developments include Aouadi's [36] formulation of a generalized linear micropolar thermoelastic model with dual relaxation times and temperature-dependent material properties. El-Karamany and Ezzat [37] introduced constitutive relations for three-phase-lag micropolar thermoelasticity, proving uniqueness, reciprocity, and variational principles for anisotropic inhomogeneous solids. Othman et al. [38] investigated the role of rotation within CD, LS, and GL-based micropolar thermoelastic models. More recently, Singh and Lianngenga [39] examined the influence of microinertia on wave motion in micropolar thermoelastic materials containing voids.

The present study analyzes the transient behavior of displacement, force stress, couple stress, and temperature fields in a two-temperature micropolar thermoelastic medium incorporating gravitational, nonlocal, and DPL effects under an inclined mechanical load. The governing equations account for initial stress and are formulated within the framework of generalized thermoelasticity. By employing normal mode analysis, exact analytical solutions for the field variables are derived. The combined influence of gravity, microstructural interactions (through nonlocality and micropolarity), two-temperature effects, and phase lags in heat conduction is examined—filling a gap in existing literature where these couplings have not been simultaneously considered.

2. Mathematical Framework

This section outlines the fundamental equations governing wave propagation in a two-temperature micropolar generalized thermoelastic medium incorporating DPL heat conduction, gravitational field, nonlocal elasticity, and initial stress effects. The model captures microstructural behavior through micropolar and nonlocal terms, while initial stress accounts for pre-existing mechanical loading in the medium. The coupled system of equations includes balance laws of linear and angular momentum, energy equation with DPL modification, constitutive relations with two-temperature dependence, and nonlocal stress-strain formulations. [40,41]

$$\sigma_{ij} = (1 - e^2\nabla^2)\sigma_{ij}^L = (\lambda u_{r,r} - \beta_1\vartheta - p)\delta_{ij} + \mu(u_{j,i} + u_{i,j}) - pw_{ij} - K(\in_{ijr} \varnothing_r - u_{j,i}), \tag{2.1}$$

$$m_{ij} = (1 - e^2\nabla^2)m_{ij}^L = \alpha\varnothing_{r,r}\,\delta_{ij} + \beta\varnothing_{i,j} + \gamma\varnothing_{j,i}\ , \tag{2.2}$$

$$\begin{aligned}\rho_0(1 - e^2\nabla^2)\frac{\partial^2 u}{\partial t^2} =&(\mu - p/2 + K)\nabla^2\overrightarrow{\mathrm{u}} + (\lambda + p/2 + \mu)\nabla(\nabla.\overrightarrow{\mathrm{u}}) \\ &+ K(\nabla \times \varnothing) + (1 - e^2\nabla^2)\overrightarrow{\mathrm{F}} - \beta_1\nabla\vartheta,\end{aligned} \tag{2.3}$$

$$\begin{aligned}\rho_j(1 - e^2\nabla^2)\frac{\partial^2\overrightarrow{\varnothing}}{\partial t^2} = (\alpha + \gamma + \beta)\nabla(\nabla.\overrightarrow{\varnothing}) - \gamma\nabla \times (\nabla \times \overrightarrow{\varnothing}) \\ - 2K\overrightarrow{\varnothing} + K(\nabla \times \overrightarrow{\mathrm{u}}),\end{aligned} \tag{2.4}$$

$$(1 + \tau_q\frac{\partial}{\partial t} + \frac{\tau_q^2}{2}\frac{\partial^2}{\partial t^2})(\rho C_*\dot{\vartheta} + \beta_1 T_0\dot{e}) = K^*(1 + \tau_T\frac{\partial}{\partial t})\nabla^2\varphi, \tag{2.5}$$

$$\varphi - \vartheta = a\nabla^2\varphi. \tag{2.6}$$

$\sigma_{ij}^L, \sigma_{ij}$ Local and nonlocal force components of stress tensor.

m_{ij}^L, m_{ij} Components of local and nonlocal couple stress tensor.

$\vec{\varnothing}$ Microrotation vector.

a Two-temperature parameter.

T, T_0 Medium and reference temperatures.

K^* Thermal conductivity.

C_E Specific heat at constant strain.

ϑ, φ Thermodynamic and conductive temperatures.

τ_T, τ_q Phase lags for temperature gradient and heat flux.

λ, μ Lamé constants.

α, K, γ, β Micropolar material constants.

j Microinertia term.

ρ Density of the medium.

u_i Components of displacement vector.

e Cubical dilation.

t Time variable.

δ_{ij} Kronecker delta.

3. Problem Description

A two-dimensional model is considered for a homogeneous, isotropic, micropolar generalized thermoelastic half-space subjected to gravitational effects, initial stress, and nonlocal interactions within the framework of two-temperature theory and the DPL model. The medium occupies the region $z \geq 0$, with the Cartesian coordinate system (x, z), where the surface $z = 0$ represents the boundary, and the z-axis is directed vertically downward. For this two-dimensional configuration, the displacement vector $\vec{u}$ and microrotation vector $\vec{\varnothing}$ are assumed as:

$$\vec{u} = (u(x, z, t), 0, w(x, z, t)), \quad \vec{\varnothing} = (0, \varnothing(x, z, t), 0). \tag{3.1}$$

The following equations are obtained by combining equations (2.3), (2.4), and (3.1).

$$\begin{aligned}\rho_0(1 - e^2\nabla^2)\frac{\partial^2 u}{\partial t^2} =&(\lambda + \mu + \frac{p}{2})\frac{\partial}{\partial x}(\frac{\partial u}{\partial x} + \frac{\partial w}{\partial z}) + (\mu + K - \frac{p}{2})(\frac{\partial^2}{\partial x^2} + \frac{\partial^2}{\partial z^2})u \\ &- K\frac{\partial \varnothing_2}{\partial z} - \beta_1\frac{\partial \vartheta}{\partial x} + (1 - e^2\nabla^2)\rho g\frac{\partial w}{\partial x},\end{aligned} \tag{3.2}$$

$$\begin{aligned}\rho_0(1 - e^2\nabla^2)\frac{\partial^2 w}{\partial t^2} =&(\lambda + \mu + \frac{p}{2})\frac{\partial}{\partial z}(\frac{\partial u}{\partial x} + \frac{\partial w}{\partial z}) + (\mu + K - \frac{p}{2})(\frac{\partial^2}{\partial x^2} + \frac{\partial^2}{\partial z^2})w \\ &+ K\frac{\partial \varnothing_2}{\partial x} - \beta_1\frac{\partial \vartheta}{\partial z} - (1 - e^2\nabla^2)\rho g\frac{\partial u}{\partial x},\end{aligned} \tag{3.3}$$

$$\rho_j(1 - e^2\nabla^2)\frac{\partial^2 \varnothing_2}{\partial t^2} = \gamma\nabla^2\varnothing_2 + K(\frac{\partial u}{\partial z} - \frac{\partial w}{\partial x}) - 2K\varnothing_2. \tag{3.4}$$

Displacement components can be expressed by using Helmholtz decomposition

$$u = \frac{\partial \psi}{\partial z} + \frac{\partial q}{\partial x}, \quad w = -\frac{\partial \psi}{\partial x} + \frac{\partial q}{\partial z}, \tag{3.5}$$

where q, ψ are scalar potential functions. By applying the expression given in Equation (3.5) to the dimensionless forms of Equations (2.5), (2.6), (3.2), and (3.4), as presented in [41], the following set of equations is derived.

$$[\nabla^2 - (1 - e^2\nabla^2)\frac{\partial^2}{\partial t^2}]q - \vartheta - (1 - e^2\nabla^2)g\frac{\partial \psi}{\partial x} = 0, \tag{3.6}$$

$$[\nabla^2 - t_1(1 - e^2\nabla^2)\frac{\partial^2}{\partial t^2}]\psi - t_2\varnothing_2 + (1 - e^2\nabla^2)gt_1\frac{\partial q}{\partial x} = 0, \tag{3.7}$$

$$[\nabla^2 - 2s_1 - s_2(1 - e^2\nabla^2)\frac{\partial^2}{\partial t^2}]\varnothing_2 + s_1\nabla^2\psi = 0, \tag{3.8}$$

$$(1 + \tau_q\frac{\partial}{\partial t} + \frac{\tau_q^2}{2}\frac{\partial^2}{\partial t^2})\frac{\partial}{\partial t}(\vartheta + \delta_0\nabla^2 q) = (1 + \tau_T\frac{\partial}{\partial t})\nabla^2\varphi, \tag{3.9}$$

$$\varphi - \vartheta = n_1\nabla^2\varphi. \tag{3.10}$$

By substituting the expression for ϑ from Equation (3.10) into Equations (3.6) and (3.9), the following modified forms of the equations are obtained.

$$[\nabla^2 - (1 - e^2\nabla^2)\frac{\partial^2}{\partial t^2}]q - (1 - e^2\nabla^2)g\frac{\partial \psi}{\partial x} + [n_1\nabla^2 - 1]\varphi = 0, \tag{3.11}$$

$$(1 + \tau_q\frac{\partial}{\partial t} + \frac{\tau_q^2}{2}\frac{\partial^2}{\partial t^2})\frac{\partial}{\partial t}[(1 - n_1\nabla^2)\varphi + \delta_0\nabla^2 q] = (1 + \tau_T\frac{\partial}{\partial t})\nabla^2\varphi. \tag{3.12}$$

4. Normal Mode Decomposition

To obtain analytical solutions, the physical field variables are expanded using normal mode analysis. Each variable is expressed as a product of a depth-dependent amplitude function and a harmonic exponential term representing wave propagation in the x-direction. The general form of the solution is:

$$\begin{aligned}&[u(x,z,t),\, w(x,z,t),\, \vartheta(x,z,t),\, \varphi(x,z,t),\, \varnothing_2(x,z,t),\\ &\quad m_{ij}(x,z,t),\, \sigma_{ij}(x,z,t)] =\\ &\quad [\tilde{u}(z),\, \tilde{w}(z),\, \tilde{\vartheta}(z),\, \tilde{\varphi}(z),\, \tilde{\varnothing}_2(z),\, \tilde{m}_{ij}(z),\, \tilde{\sigma}_{ij}(z),] \cdot e^{\omega t + ivx}\end{aligned} \tag{4.1}$$

where $\tilde{u}(z), \tilde{w}(z), \tilde{\theta}(z), \ldots$ denote the amplitude functions varying with depth z, ω is the angular frequency, $i = \sqrt{-1}$ is the imaginary unit, and v is the wave number in the x-direction.

Substituting the solutions given in Equation (4.1) into Equations (3.7), (3.8), (3.11), and (3.12), we obtain the following four equations.

$$[O_1(D^2 - v^2) - \gamma_1]\tilde{\varphi} - O_2[D^2 - v^2]\tilde{q} = 0, \tag{4.2}$$

$$[F_1 D^2 - O_3]\tilde{q} - [1 - n_1(D^2 - v^2)]\tilde{\varphi} - O_4\tilde{\psi} = 0, \tag{4.3}$$

$$[F_2 D^2 - O_5]\tilde{\psi} - t_2\tilde{\varnothing}_2 + O_6\tilde{q} = 0, \tag{4.4}$$

$$[F_3 D^2 - O_7]\tilde{\varnothing}_2 + [s_1(D^2 - v^2)]\tilde{\psi} = 0. \tag{4.5}$$

Solving Equations (4.2)–(4.5) simultaneously yields an eighth-order differential equation.

$$(D^8 + L_1 D^6 + L_2 D^4 + L_3 D^2 + L_4)(\tilde{\psi}, \tilde{\varnothing}_2, \tilde{q}, \tilde{\varphi}) = 0 \tag{4.6}$$

This equation is then solved to obtain the eigenvalues $k_i^2 (i = 1, 2, 3, 4)$ for characteristic equation $(k^8 + L_1 k^6 + L_2 k^4 + L_3 k^2 + L_4) = 0$. The solutions of Equation (4.6) that remain bounded as $z \to \infty$, in accordance with the radiation condition, are given by:

$$(\tilde{\psi}_{(r=0)}, \tilde{\varnothing}_{2(r=1)}, \tilde{q}_{(r=2)}, \tilde{\varphi}_{(r=3)})(z) = \sum_{n=1}^{4} E_{rn} M_n(v, w) e^{-k_n z}. \tag{4.7}$$

Stresses and microrotational factor can be represented using (2.1), (2.2), and (3.1) as

$$\sigma_{zz} = (1 - e^2\nabla^2)\sigma_{zz}^L = \frac{\partial^2 q}{\partial z^2} + P_1 \frac{\partial^2 \psi}{\partial z \partial x} + P_2 \frac{\partial^2 q}{\partial x^2} - (1 - n_1\nabla^2)\varphi - P_0, \tag{4.8}$$

$$\sigma_{zx} = (1 - e^2\nabla^2)\sigma_{zx}^L = P_3 \frac{\partial^2 q}{\partial z \partial x} - P_4 \frac{\partial^2 \psi}{\partial x^2} + P_5 \frac{\partial^2 \psi}{\partial z^2} - P_6 \varnothing_2, \tag{4.9}$$

$$m_{zy} = (1 - e^2\nabla^2) m_{zy}^L = \delta_1 \frac{\partial \varnothing_2}{\partial z}. \tag{4.10}$$

By utilizing the non-dimensional variables along with the expressions from Equation (3.5), and substituting them into Equations (4.8)–(4.10), the stress components are derived in the following form:

$$\tilde{\sigma}_{zz} = (D^2 - v^2 P_2)\tilde{q} + \iota v P_1 D\tilde{\psi} + (n_1(D^2 - v^2) - 1)\tilde{\varphi} - P_0, \tag{4.11}$$

$$\tilde{\sigma_{zx}} = \iota v P_3 D\tilde{q} + (P_4 v^2 + P_5 D^2)\tilde{\psi} - P_6\tilde{\varnothing}_2, \tag{4.12}$$

$$\tilde{m}_{zy} = \delta_1 D\tilde{\varnothing}_2, \tilde{w} = D\tilde{q} - \iota v\tilde{\psi}, \tilde{u} = \iota v\tilde{q} + D\tilde{\psi}. \tag{4.13}$$

By substituting the solution from Equation (4.7) into Equations (4.11)–(4.13) and (3.10), these equations can be reformulated as follows:

$$\begin{aligned}&(\tilde{\sigma}_{zz(r=6)}, \tilde{\sigma}_{zx(r=5)}, \tilde{m}_{zy(r=4)}, \tilde{u}_{(r=7)}, \tilde{w}_{(r=8)}, \tilde{\vartheta}_{(r=9)})\\ &= \sum_{n=1}^{4} E_{rn} M_n(v, w) e^{-k_n z} - s_r P_0.\end{aligned} \tag{4.14}$$

5. Application of Inclined Load

A homogeneous, isotropic, micropolar generalized thermoelastic medium with nonlocal elasticity, initial stress, gravity, and two-temperature effects occupying the region $z \geq 0$ is considered. The boundary $z = 0$ is subjected to an inclined line load $F0$ at angle θ to the z-axis:

$$F1 = F0 \sin\theta, \quad F2 = F0 \cos\theta,$$

where $F1$ and $F2$ represent tangential and normal components. The surface also sustains an initial compressive stress P_0.
The boundary conditions (on surface) $z = 0$ are:

$$\sigma_{zz} + P_0 = -F2\delta(x)H(t), \tag{5.1}$$
$$\sigma_{zx} = -F1\delta(x)H(t), \tag{5.2}$$
$$\varphi = 0, \tag{5.3}$$
$$m_{zy} = 0, \tag{5.4}$$

where $\delta(x)$ is the Dirac delta function and $H(t)$ is the Heaviside unit step function.
Using normal mode analysis, the frequency domain boundary conditions become

$$\bar{\sigma}_{zz} = \frac{-F0\cos\theta}{\omega} - P_0, \tag{5.5}$$
$$\bar{\sigma}_{zx} = \frac{-F0\sin\theta}{\omega}, \tag{5.6}$$
$$\bar{\varphi} = 0, \tag{5.7}$$
$$\bar{m}_{zy} = 0. \tag{5.8}$$

Equations (4.14) for r = 4, 5, 6, and Equation (4.7) for r=3 are transformed into a non-homogeneous

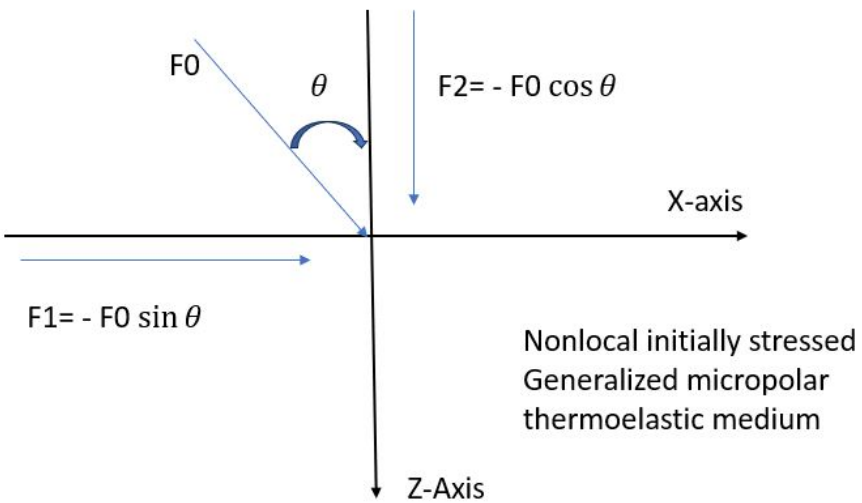

Figure 1: Schematic of inclined line load $F0$ on the surface of a nonlocal micropolar thermoelastic medium.

system of equations through the application of the boundary conditions described above.

$$\begin{bmatrix} E_{61} & E_{62} & E_{63} & E_{64} \\ E_{51} & E_{52} & E_{53} & E_{54} \\ E_{41} & E_{42} & E_{43} & E_{44} \\ E_{31} & E_{32} & E_{33} & E_{34} \end{bmatrix} \begin{bmatrix} M_1 \\ M_2 \\ M_3 \\ M_4 \end{bmatrix} = \begin{bmatrix} R_1 \\ R_2 \\ 0 \\ 0 \end{bmatrix} \tag{5.9}$$

where

$$R_1 = \frac{-F0\cos\theta}{w} - P_0,\ R_2 = \frac{-F0\sin\theta}{w}.$$

The coefficients $M_n, n = 1, 2, 3, 4.$ can be determined from Equation (5.9) using Cramer's rule. Substituting these values into Equations (4.7) and (4.14) yields the following results:

$$(\tilde{\psi}_{(r=0)}, \tilde{\varnothing}_{2(r=1)}, \tilde{q}_{(r=2)}, \tilde{\varphi}_{(r=3)}, \tilde{m}_{zy(r=4)},$$
$$\tilde{\sigma}_{zx(r=5)}, \tilde{\sigma}_{zz(r=6)}, \tilde{u}_{(r=7)}, \tilde{w}_{(r=8)}, \tilde{\vartheta}_{(r=9)})(z) = \frac{1}{\Delta}\sum_{n=1}^{4}\Delta_n E_{rn} e^{-k_n z}. \tag{5.10}$$

6. Numerical Illustration

To investigate the effects of nonlocality, two-temperature parameters, initial stress, and inclination angle on field variables in the medium, a numerical analysis is performed. The material properties used for the computations correspond to a magnesium crystal-like solid and are listed in Table 1, (see [7]).

The field equations are solved numerically for various values of the inclination angle θ, two-temperature

Table 1: Material constants for a magnesium crystal-like medium

Parameter	**Value**
Mass density, ρ	1.74×10^3 kg m^{-3}
Lame's constant, λ	9.4×10^{10} kg m^{-1}s^{-2}
Shear modulus, μ	4.0×10^{10} kg m^{-1}s^{-2}
Thermal conductivity, k	1.0×10^{10} kg m^{-1}s^{-2}
Thermal modulus, γ	0.779×10^{-9} kg m s^{-2}
Microinertia, j	0.2×10^{-19} m^2
Thermal conductivity*, k^*	2.510 W m^{-1}K^{-1}
Nonlocal parameter, a	0.074×10^{-15} m^2
Specific heat, C_E	9.623×10^2 J kg^{-1} K^{-1}
Thermal expansion, α_t	2.36×10^{-5} K^{-1}
Initial temperature, T_0	293 K
Phase lag (heat flux), τ_q	0.2 s
Phase lag (temperature gradient), τ_T	0.15 s

parameter a, and nonlocality along with the effect of the gravitational feild to investigate their combined effects on the displacement, stress, temperature, and microrotation profiles within the medium.

The analytical solution expressed in Equation (4.1) contains $e^{(\omega t + \iota v x)}$ (exponential term), where the angular frequency ω is generally complex ($\omega = \omega_0 + \iota\omega_1$) . Hence, the time-dependent part becomes:

$$e^{\omega t} = [\cos(\omega_1 t) + \iota \sin(\omega_1 t)]\, e^{\omega_0 t}.$$

For small time intervals, the imaginary part ω_1 has a negligible effect; thus, ω may be assumed real ($\omega = \omega_0$) for simplification in numerical computations.

In the current analysis, the values of frequency and wave number are chosen as $\omega = 1.0$ and $v = 1.2$, respectively. Using the material parameters listed previously, the field variables have been computed and plotted as functions of depth (z) at a fixed instant $t = 0.01$ and lateral position $x = 1.0$.

7. Graphical Interpretation of Results

For interpretative clarity and application relevance, the graphical results are categorized into two main sets:

Set I: Effect of Pre-stress and Two Temperature

Figures 2 - 11 illustrate the behavior of the field variables under the combined influence of prestress and the two-temperature parameter. The two curves (solid blue and magenta with markers) represent a comparison of different initial stress values, p = 5 and p = 9, under two-temperature theory, demonstrating how increased initial stress affects field behavior in the presence of thermal coupling. The two curves (magenta with markers and black dashed) correspond to a fixed initial stress value (p=9), allowing a direct comparison between the two-temperature model (a=0.074) and the classical single-temperature theory (a=0). This highlights the influence of thermal modeling on the response of the field variable. This setup enables a comparative understanding of how field variables respond to both the variation in initial stress and the transition between single- and two-temperature theories.

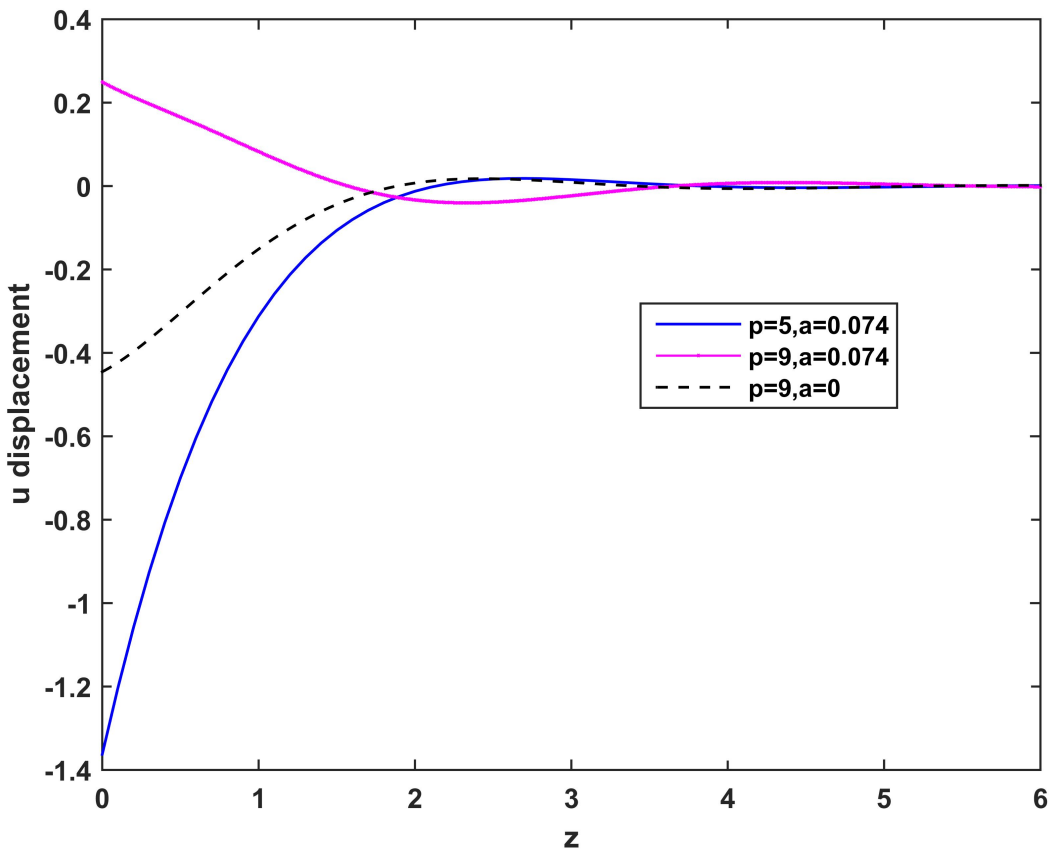

Figure 2: Variation of horizontal displacement U for initial stress and two temperature parameter

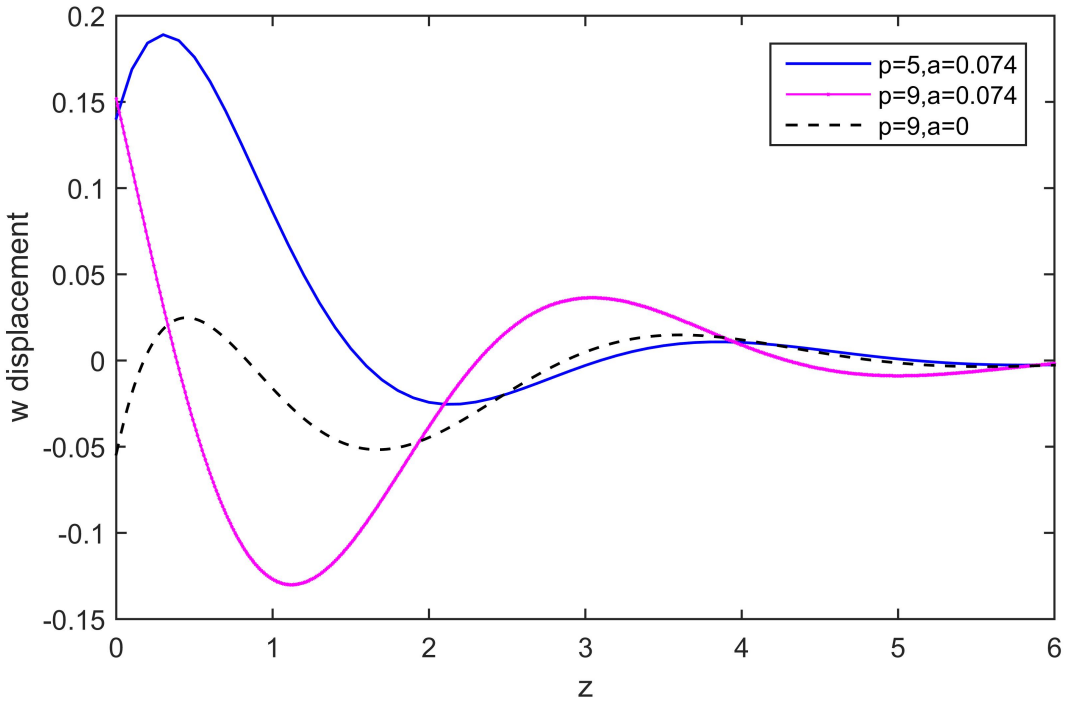

Figure 3: Variation of vertical displacement W for initial stress and two temperature parameter

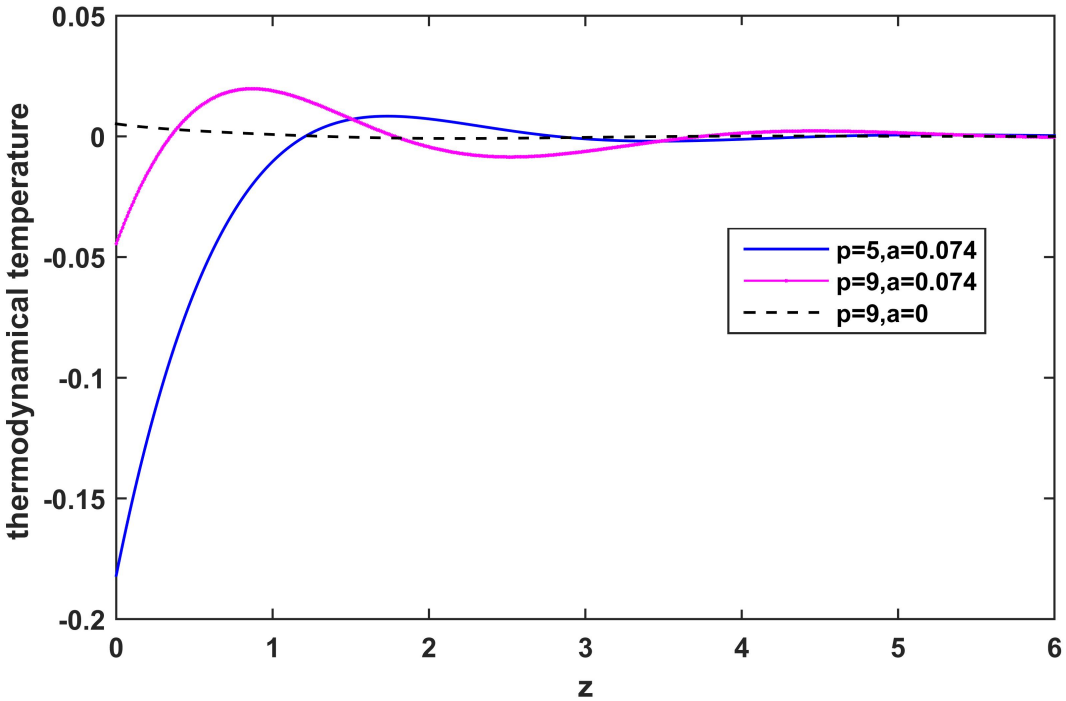

Figure 4: Variation of thermodynamic temperature ϑ for initial stress and two temperature parameter

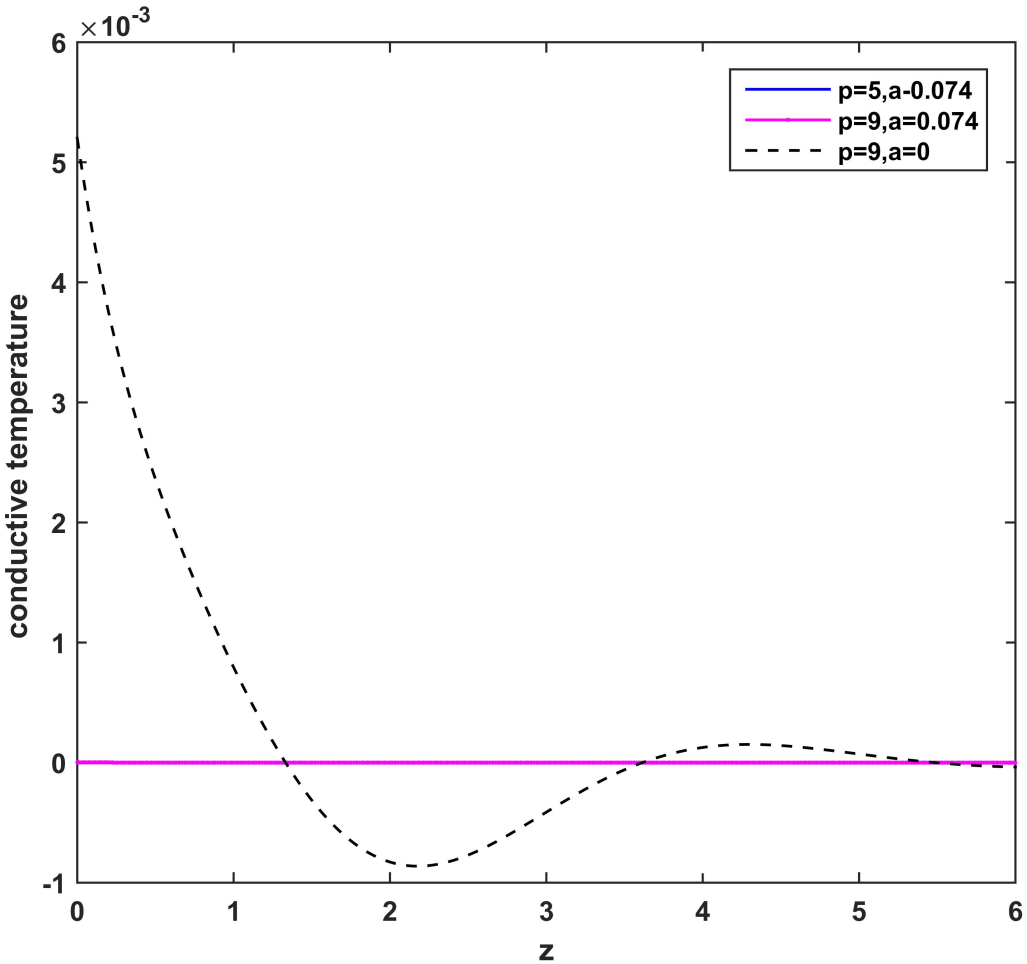

Figure 5: Variation of conductive temperature φ for initial stress and two temperature parameter

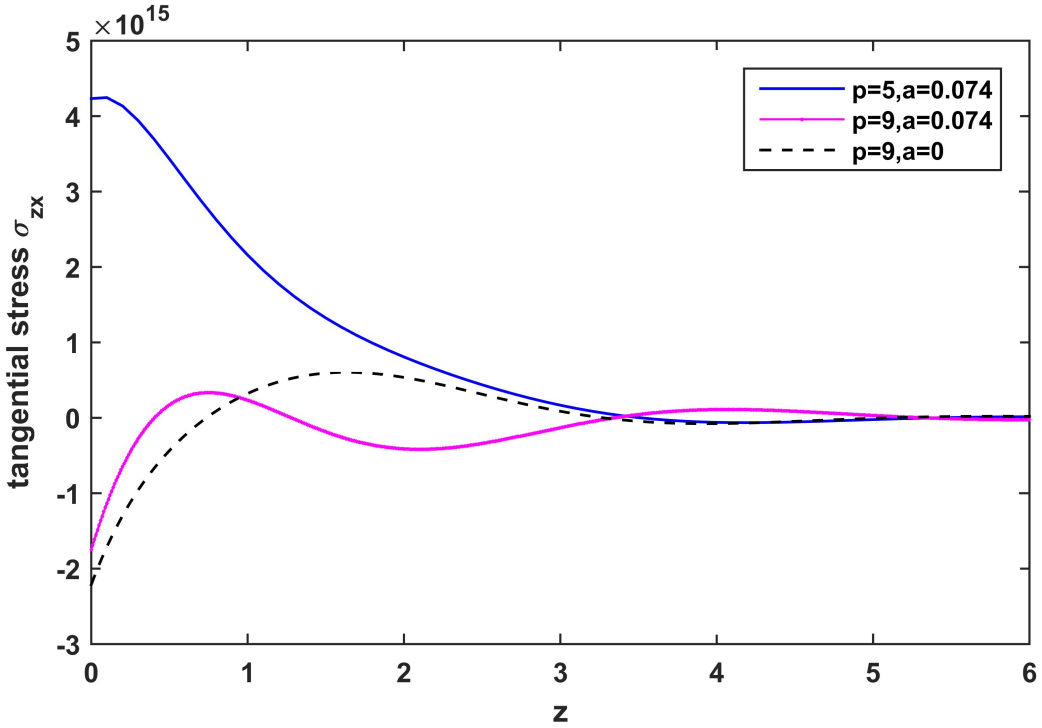

Figure 6: Variation of tangential stress σ_{zx} for initial stresses and two temperature parameter

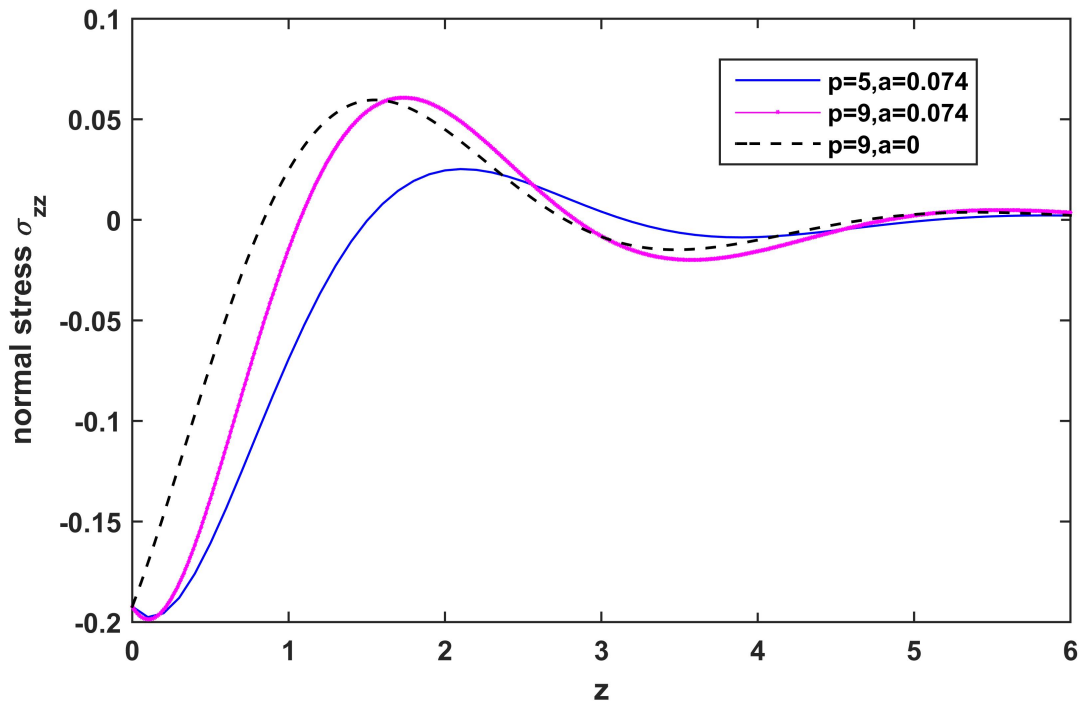

Figure 7: Variation of normal stress σ_{zz} for initial stresses and two temperature parameter

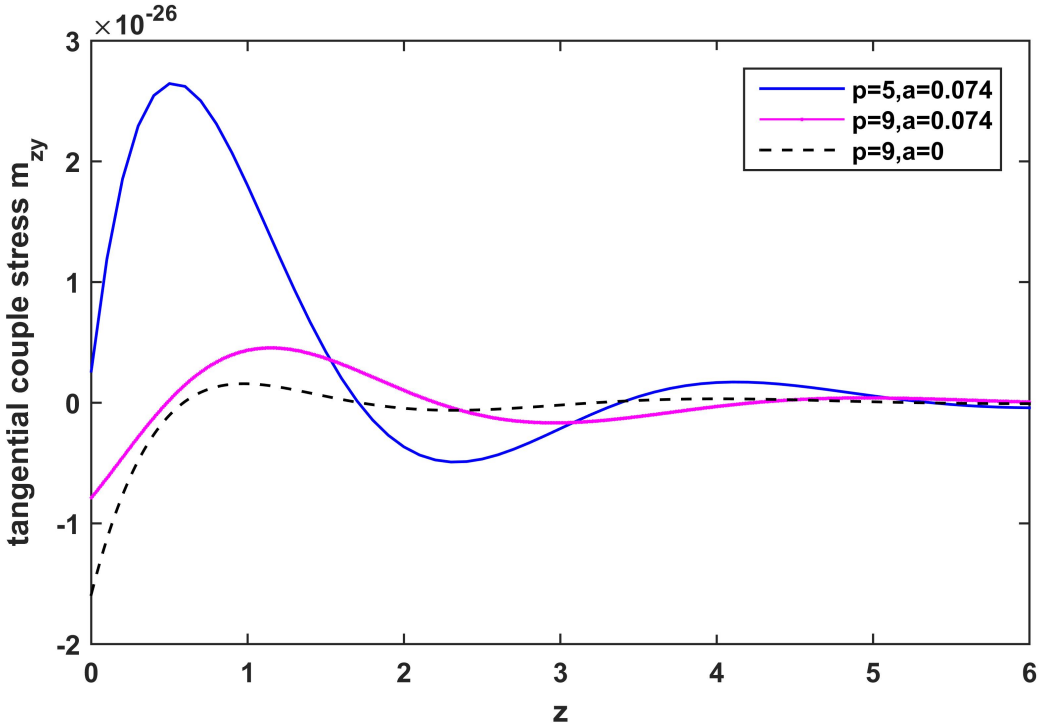

Figure 8: Variation of couple stress m_{zy} for initial stresses and two temperature parameter

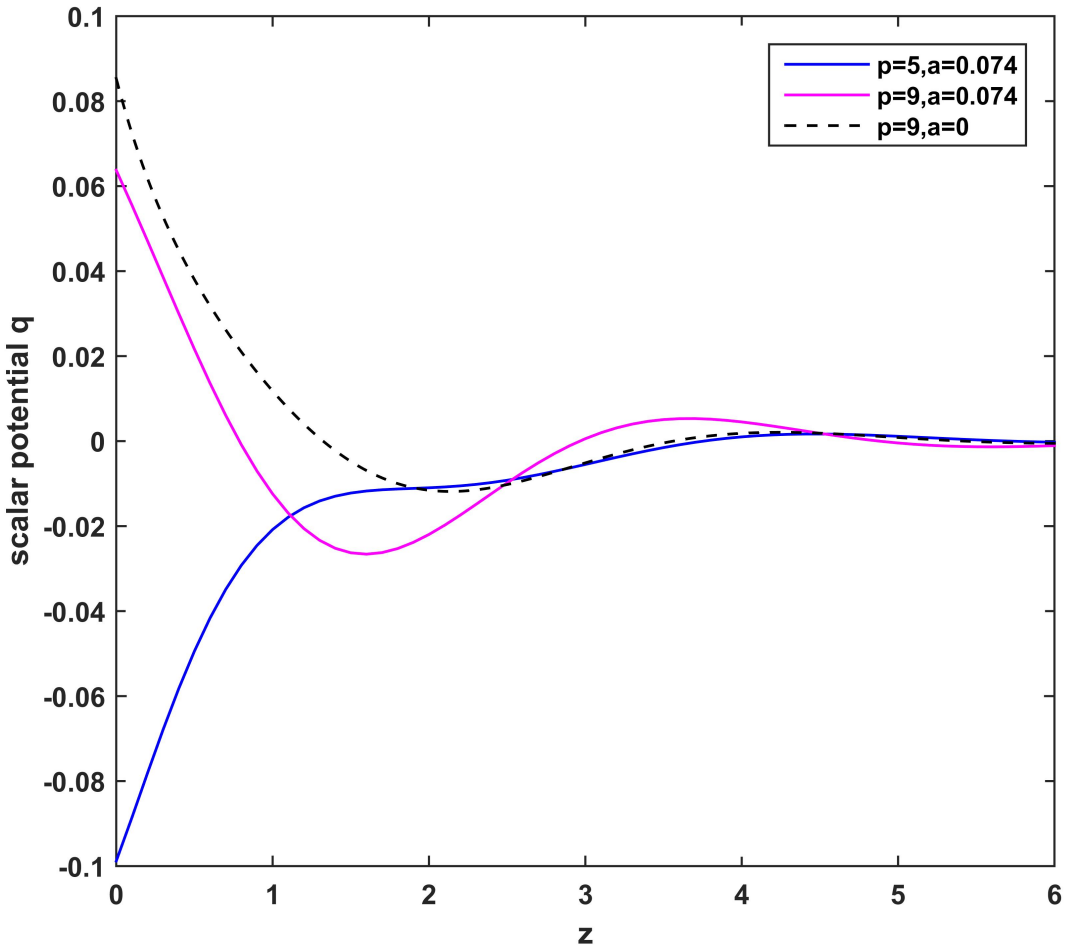

Figure 9: Variation of scalar potential q for initial stresses and two temperature parameter

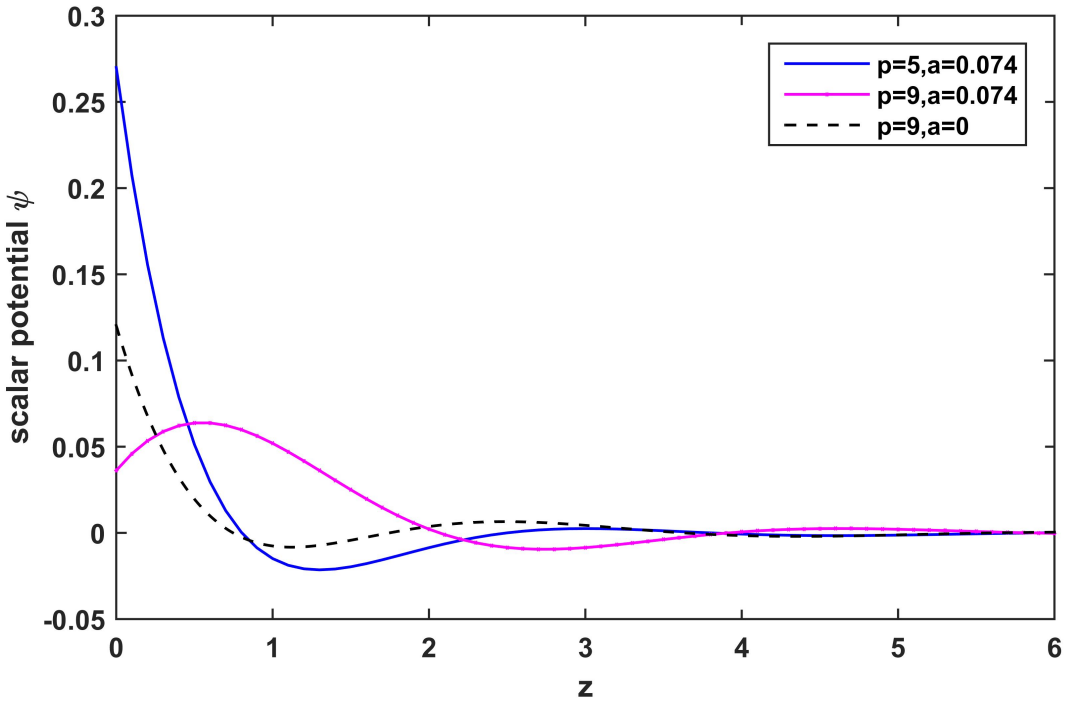

Figure 10: Variation of scalar potential ψ for initial stresses and two temperature parameter

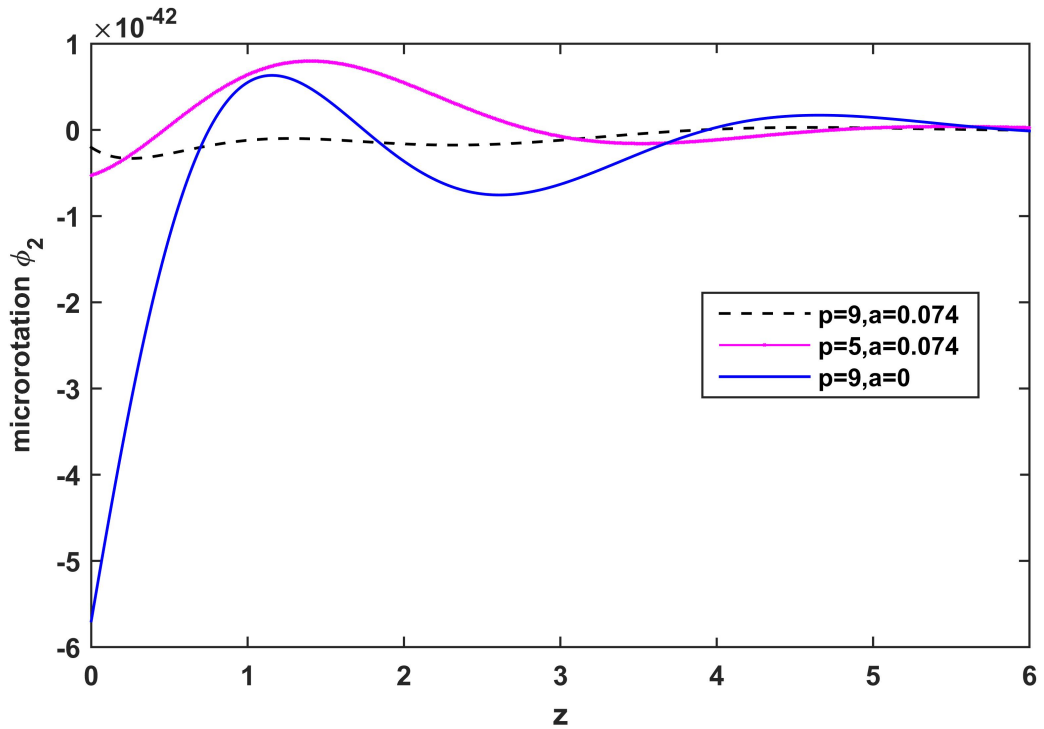

Figure 11: Variation of microrotation $\varnothing_2$ for initial stresses and two temperature parameter

Set II: Effect of nonlocality and load inclination

The graphical results for the physical variables (Figures 12 - 21) illustrate the combined influence of the non-local parameter e and the angle of inclination θ of the applied mechanical load on the dynamic response of the material. Each plot comprises four representative curves that enable a comparative interpretation of these effects. In particular, the solid blue and solid black curves highlight the influence of varying the nonlocal parameter e, while maintaining a fixed inclination angle ($\theta = 45$). These curves allow one to examine how nonlocality intensifies or modulates the field behavior. An increase in e is observed to enhance the amplitude and spatial spread of responses across all physical fields, reflecting the extended interaction range inherent to nonlocal elasticity.
In contrast, the solid black, dashed red, and dashed magenta lines correspond to a fixed non-local parameter (e = 0.9) but vary the angle of inclination of the applied mechanical load, with $\theta = 45, 90, 0$, respectively. These curves reveal the directional sensitivity of the physical fields. Notably,($\theta = 90$), representing a normal load, leads to different magnitudes and gradients in the responses compared to oblique or tangential loads ($\theta = 45, 0$), indicating anisotropic mechanical behavior under varying load orientations.
In summary, the figures collectively demonstrate that both the non-local parameter and the angle of applied load significantly influence the propagation and intensity of the field variables. While the non-local parameter e governs the scale and dispersive nature of the response, the inclination angle θ modulates its directionality and magnitude. Such interactions are critical for understanding the mechanical behavior of micro- and nanoscale structures, where nonlocal effects and load orientation are nonnegligible and can substantially alter system performance.

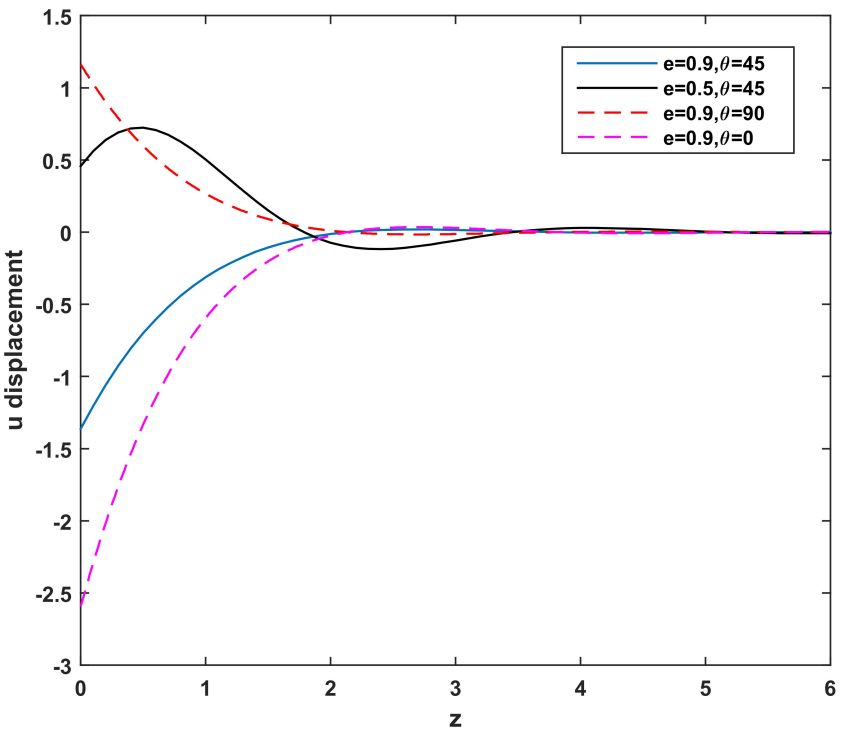

Figure 12: Variation of horizontal displacement U for nonlocality and inclined angle

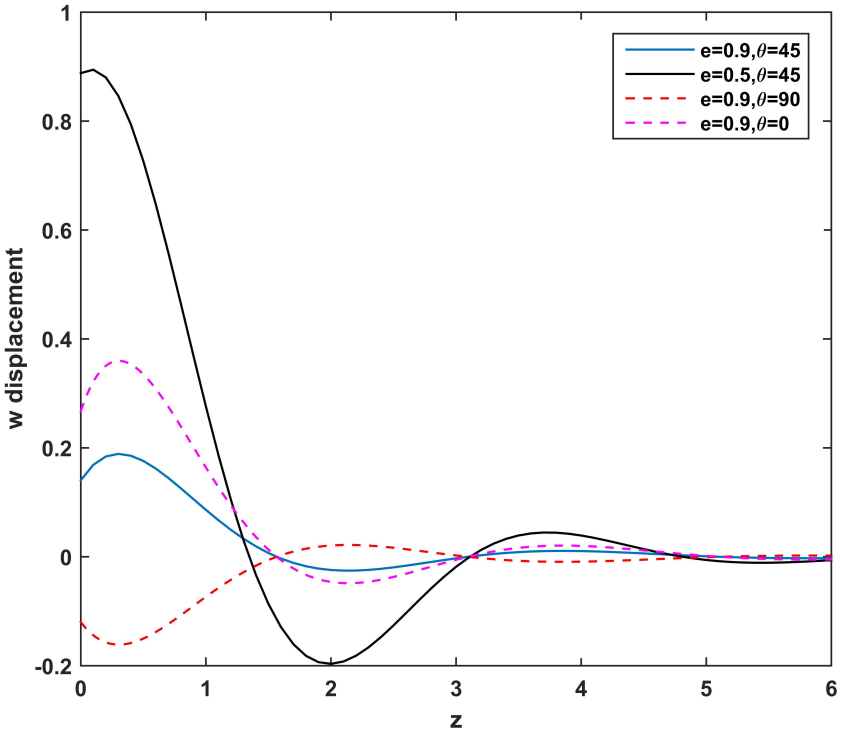

Figure 13: Variation ofvertical displacement W for nonlocality and inclined angle

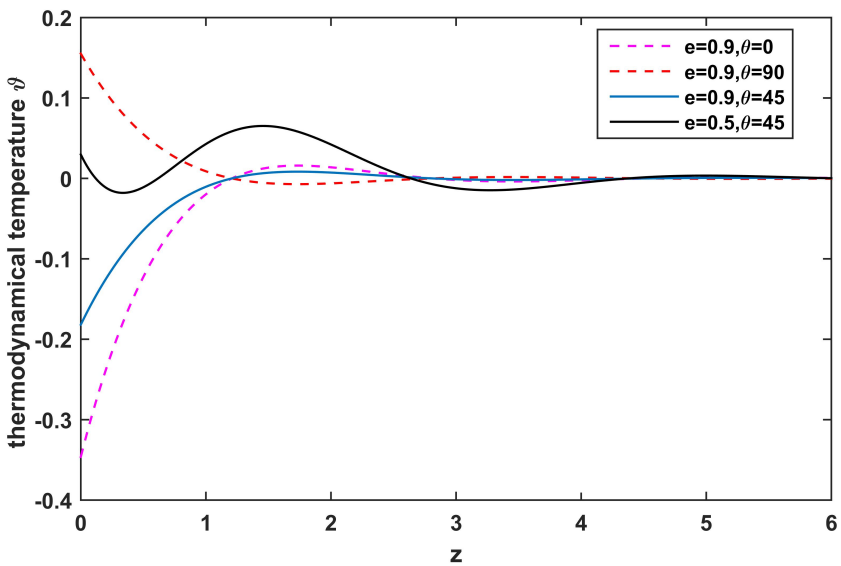

Figure 14: Variation of thermodynamic temperature ϑ for nonlocality and inclined angle

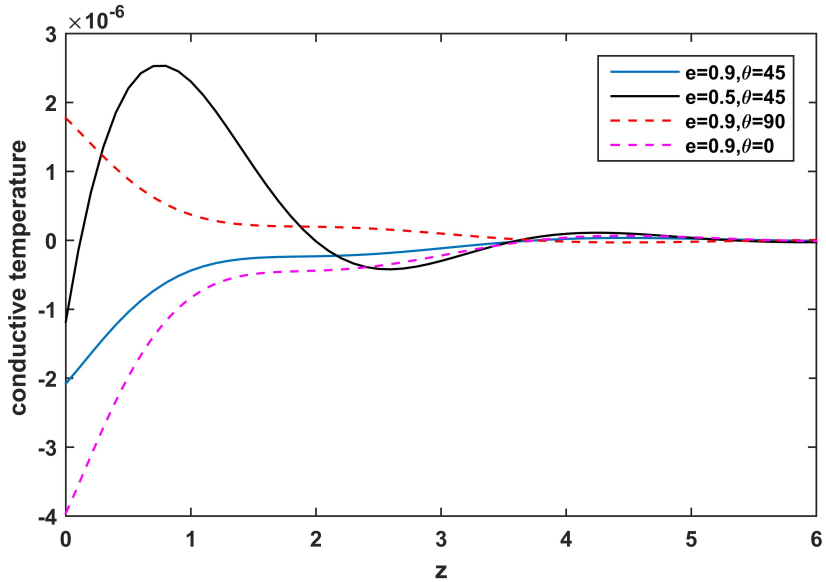

Figure 15: Variation ofconductive temperature φ for nonlocality and inclined angle

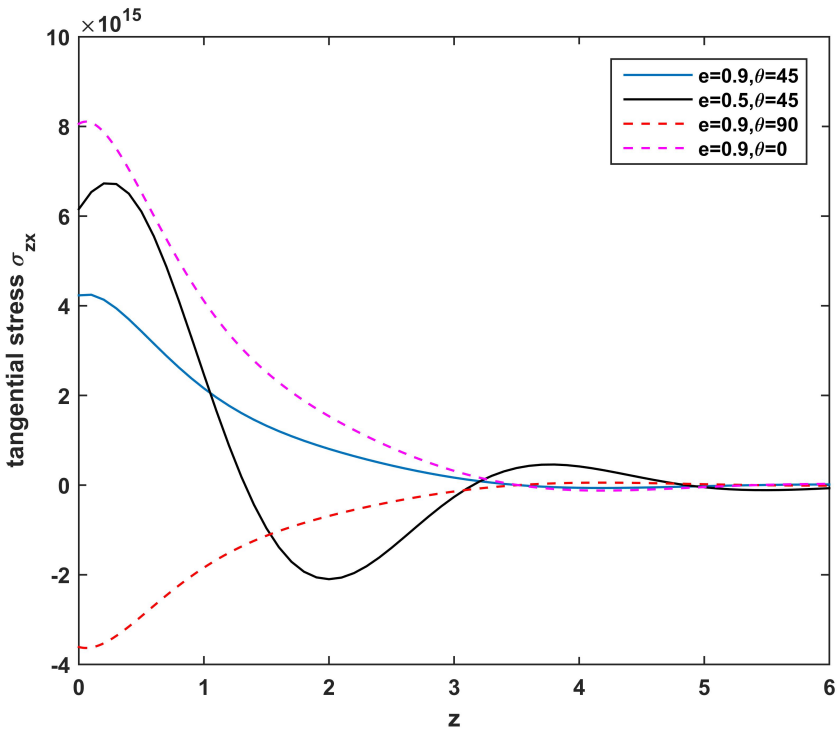

Figure 16: Variation of tangential stress σ_{zx} for nonlocality and inclined angle σ_{zx}

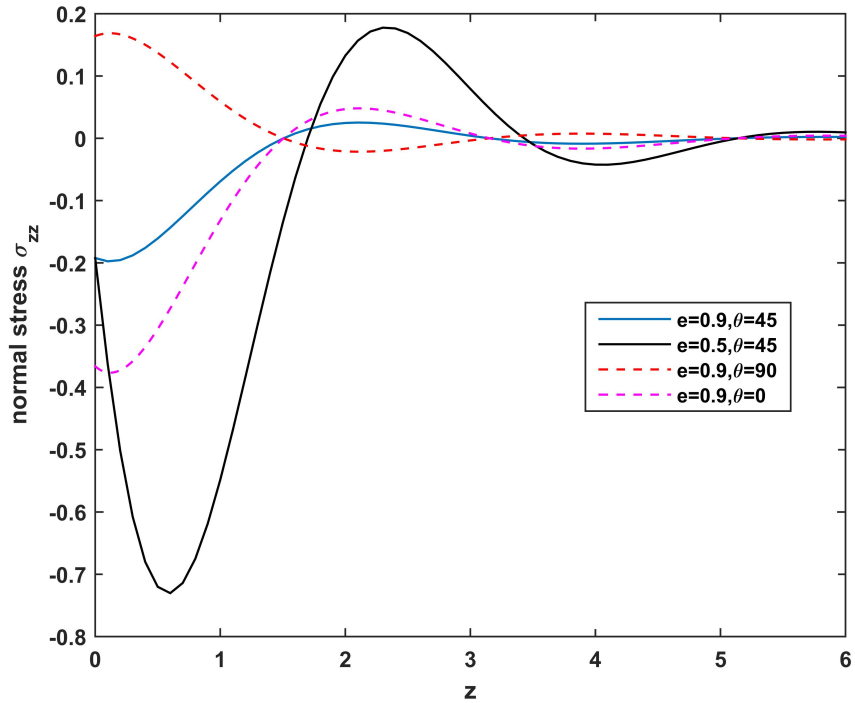

Figure 17: Variation of normal stress σ_{zz} for nonlocality and inclined angle

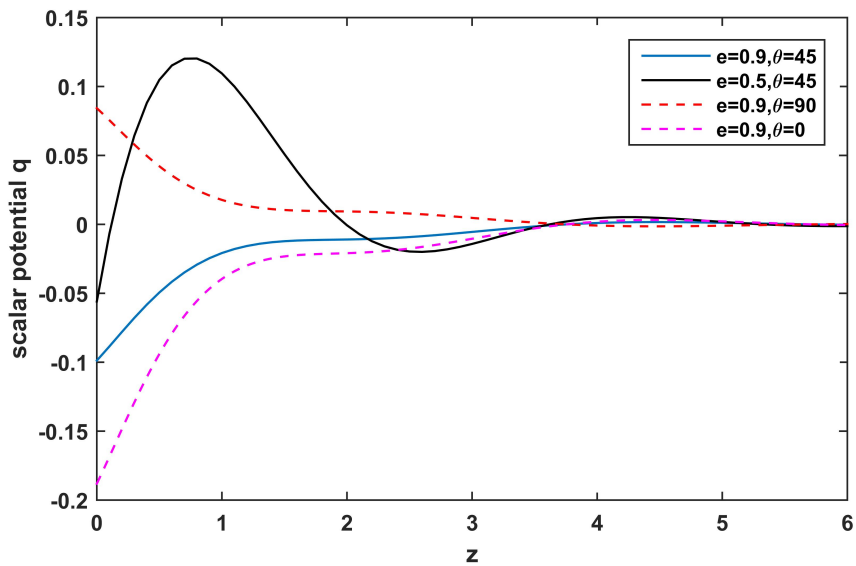

Figure 18: Variation of scalar potential q for nonlocality and inclined angle

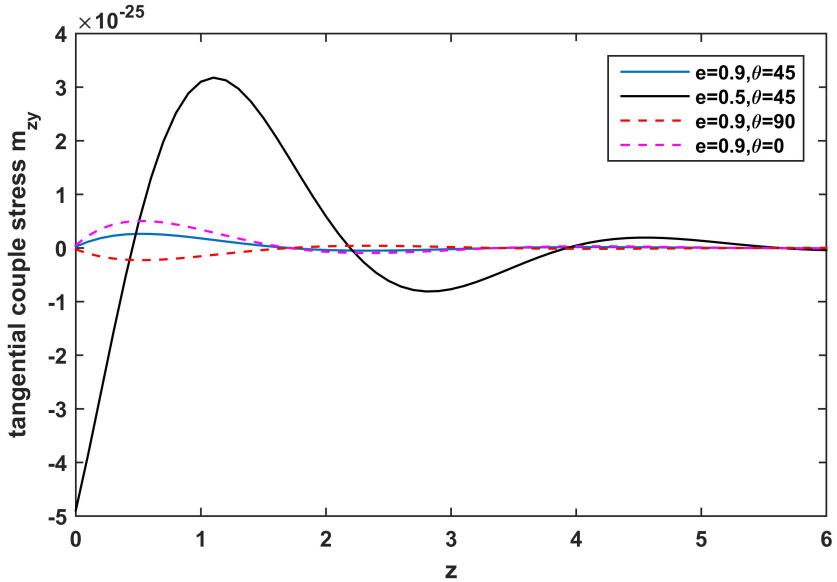

Figure 19: Variation of couple stress m_{zy} for nonlocality and inclined angle

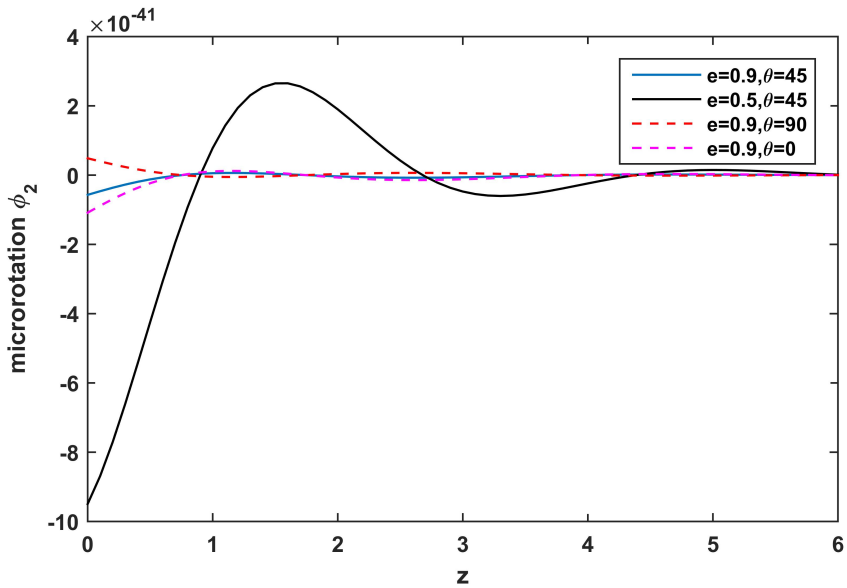

Figure 20: Variation of scalar potential ∅ for nonlocality and inclined angle

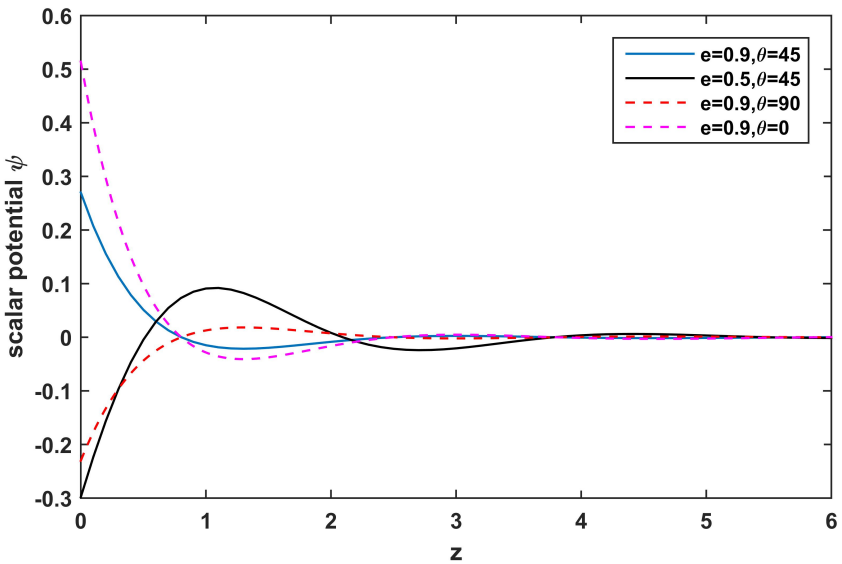

Figure 21: Variation of microrotation ψ for nonlocality and inclined angle

Special Cases

Case I: Neglecting the effect of nonlocal and initial stress ($e = 0$ and $p = 0$).
Assuming nonlocal factor $e = 0$ and initial stress $p = 0$, the outcomes of the present problem are the same as obtained by Deswal [41]
Case II: Without Gravity ($g = 0$)
Furthermore, if the effect of gravity is neglected in the medium(g=0), the system reduces to the same as the special Case I in the study given by Deswal [41]
Case III: Considering one temperature ($\vartheta = \varphi$)
Considering thermodynamic temperature equal to conductive temperature for the discussed problem along with the above two cases, the medium under study is reduced to one temperature problem, and the output will become as of Othman and Singh [42] in his research implement alterations to loading and boundary conditions while excluding rotational effects.

8. Conclusion

The analysis of the behavior of stress components, displacement, and temperature in an isotropic, homogeneous, non-local, micropolar thermoelastic medium with gravity, two temperature and initial stress in the context of the DPL theory. Numerical and theoretical outcome reveal that parameter namely the angle of inclination of load, gravity, two temperature, and initial stress,s have a significant effect on the physical variables under study. The following are the concluding points:
(1) Variation of all the fields is in a limited region, which support the physical facts and notion of generalised thermoelasticity theory.
(2) Nonlocal effects considerably influence all the field variables under investigation, while variations in the angle of inclination of the applied load (θ) affect most of the field responses; the microrotation and tangential couple stress components exhibit only minor variations in comparison to the other fields. (Figure 2 - 11)
(3) A significant effect of initial stress on all physical quantities under the two-temperature theory, with the exception of the conductive temperature, which remains relatively unaffected, is observed. Furthermore, a comparative analysis between the two-temperature model and the classical one-temperature theory (a=0) clearly highlights the influence of the two-temperature parameter on the overall behavior of the system. (Figure 12 -21)

(4) As intended, all physical quantities meet the boundary conditions.

The significance of this problem becomes apparent when considering the actual behavior of materials and the suitable geometry of the model. Precious materials, fluid-like substances, such as Petroleum products and oils exist in crude form within the Earth, while the rocks or materials surrounding them are often granular. The crude fluids and granular rocks can be effectively modeled using the micropolar theory of thermoelasticity. This field finds applications in seismic engineering, nanoscale materials, composite materials, biological tissue, geomechanics, structural health monitoring, earthquake engineering, and related areas.

Acknowledgments

We thank the organizers of the "International Conference on Mathematical Sci- ences and Computing Innovations and Applications" (ICMSC-2025) jointly or- ganized by Department of Mathematics North Eastern Regional Institute of Science and Technology (NERIST) and Department of Mathematics National institute of technology (NIT), Uttarakhand held over June 26-28, 2025.

Appendix

$$
\begin{aligned}
D =&\frac{d}{dz},\\
O_1 =&1+\gamma_1 n_1, \quad O_2=\gamma_1\delta_0, \quad O_4=\iota g v,\\
O_3 =&v^2+w^2+e^2w^2, \quad O_6=\iota(gvt_1),\\
O_5 =&v^2+t_1w^2+t_1w^2e^2v^2,\\
O_7 =&v^2+2s_1+s_2w^2+s_2e^2v^2w^2,\\
F_1 =&1+e^2w^2, \quad F_2=1+t_1e^2w^2, \quad F_3=1+s_2e^2w^2,\\
t_1 =&\frac{\rho c_1^2}{(\mu+K-\frac{p}{2})}, \quad t_2=\frac{K}{(\mu+K-\frac{p}{2})},\\
s_1 =&\frac{Kc_1^2}{\gamma w^{*2}}, \quad s_2=\frac{\rho_j c_1^2}{\gamma}, \quad n_1=\frac{aw^{*2}}{c_1^2}, \quad \delta_0=\frac{\beta_1^2 T_0}{\rho w^* K^*},\\
\gamma_1 =&\frac{(1+\tau_q w+\frac{\tau_q^2}{2}w^2)w}{1+\tau_T w},\\
S_{1_1} =&F_2F_3, \quad S_{2_2}=-O_7F_2-O_5F_3+s_1t_2,\\
S_3 =&O_5O_7-M^2s_1t_2, \quad T_1=-n_1S_{1_1},\\
T_2 =&(1-v^2)S_{1_1}-n_1S_{2_2}, \quad T_3=(1-v^2)S_{2_2}-n_1S_3,\\
T_4 =&(1-v^2)S_3, \quad S_4=S_{1_1}F_1, \quad S_5=-O_3S_{1_1}+F_1S_{2_2},\\
S_6 =&-O_3S_{2_2}+F_1S_3-O_6O_4F_3, \quad S_7=-O_3S_3+O_7O_4O_6,\\
S_8 =&-(v^2O_1+\gamma_1),\\
V_1 =&O_1S_4-O_2T_1, \quad V_5=O_2v^2T_4+S_7S_8,\\
V_2 =&O_2v^2T_1-O_2T_2+S_8S_4+O_1O_5,\\
V_4 =&O_2v^2T_3-O_2T_4+O_1S_7+S_8S_6,\\
V_3 =&v^2O_2T_2-O_2T_3+S_5S_8+O_1S_6,\\
L_1 =&\frac{V_2}{V_1}, \quad L_4=\frac{V_5}{V_1}, \quad L_3=\frac{V_4}{V_1}, \quad L_2=\frac{V_3}{V_1},\\
E_{1n} =&\frac{-s_1(k_n^2-v^2)}{F_3k_n^2-O_7},
\end{aligned}
$$

$$
\begin{aligned}
E_{2n} =& \frac{t_2 E_{1n} - (F_2 k_n^2 - O_5)}{O_6},\\
E_{0n} =& 1, \quad E_{3n} = \frac{O_2(k_n^2 - v^2)E_{2n}}{O_1(k_n^2 - v^2) - \gamma_1},\\
P_0 =& \frac{p}{\beta_1 T_0}, \quad P_1 = \frac{-(2\mu + K)}{\lambda + K + 2\mu}, \quad P_2 = \frac{\lambda}{\lambda + K + 2\mu},\\
P_3 =& \frac{(2\mu + K)}{\rho c_1^2}, \quad P_4 = \frac{\mu - \frac{p}{2}}{\rho c_1^2}, \quad P_5 = \frac{\mu + K + \frac{p}{2}}{\rho c_1^2},\\
P_6 =& \frac{K}{\rho c_1^2}, \quad \delta_1 = \frac{\gamma C_* w^*}{K^* c_1^2},\\
s_r =& \begin{cases} 1, & \text{for } r = 6,\\ 0, & \text{otherwise,} \end{cases}\\
E_{4n} =& - k_n \delta_1 E_{1n},\\
E_{5n} =& - ivP_3 k_n E_{2n} + P_4 v^2 + k_n^2 P_5 - P_6 E_{1n},\\
E_{6n} =& k_n^2 E_{2n} - k_n ivP_1 - v^2 P_2 E_{2n} - E_{3n} + n_1 E_{3n}(k_n^2 - v^2),\\
E_{7n} =& ivE_{2n} - k_n, \quad E_{8n} = -k_n E_{2n} - iv, \quad E_{9n} = E_{3n} - n_1 E_{3n}(k_n^2 - v^2).
\end{aligned}
$$

References

1. Lord, H. W., Shulman, Y., *a generalized dynamical theory of thermoelasticity*, J. Mech. Phys. Solids 15, 299–309, (1967).
2. Green, A. E., Lindsay, K. A., *thermoelasticity*, J. Elasticity 2, 1–7, (1972).
3. Green, A. E., Naghdi, P. M., *thermoelasticity without energy dissipation*, J. Elasticity 31, 189–208, (1993).
4. Tzou, D. Y., *a unified field approach for heat conduction from macro- to micro-scales*, J. Heat Transfer 117, 8–16, (1995).
5. Ragab, M., Abo-Dahab, S. M., Abouelregal, A. E., Kilany, A. A., *a thermoelastic piezoelectric fixed rod exposed to an axial moving heat source via a dual-phase-lag model*, Complexity 2021, 5547566, (2021).
6. Peng, W., Qi, Z., He, T., *nonlocal dual-phase-lag thermoviscoelastic response of a polymer microbeam incorporating modified couple stress and fractional viscoelastic theories*, J. Strain Anal. Eng. Des. 58, 376–388, (2023).
7. Bajaj, S., Shrivastav, A. K., Kumari, S., *effect of nonlocal micropolar thermoelasticity with initial stress in the context of dual phase lag in thermodynamical interactions*, in Proc. 2024 Int. Conf. Control, Comput., Commun. Mater. (ICCCCM), 494–501, (2024).
8. Srivastava, A., Mukhopadhyay, S., *vibration analysis of a transversely isotropic piezothermoelastic beam resonators under nonlocal strain gradient theory with dpl model*, Acta Mech. 1–20, (2025).
9. Abouelregal, A. E., Alhassan, Y., Althagafi, H., Alsharif, F., *a two-temperature fractional dpl thermoelasticity model with an exponential rabotnov kernel for a flexible cylinder with changeable properties*, Fractal Fract. 8, 182, (2024).
10. Youssef, H. M., Al-Lehaibi, E. A., *the vibration of viscothermoelastic static pre-stress nanobeam based on two-temperature dual-phase-lag heat conduction and subjected to ramp-type heat*, J. Strain Anal. Eng. Des. 58, 410–421, (2023).
11. Chen, P., Gurtin, M. E., *on a theory of heat conduction involving two temperatures*, Z. Angew. Math. Phys. (ZAMP) 19, 614–627, (1968).
12. Chen, P., Gurtin, M. E., *heat conduction in deformable bodies*, Int. J. Eng. Sci. 6, 529–545, (1968).
13. Chen, P., Gurtin, M. E., Liu, W. T., *a general theory of heat conduction with two temperatures*, Arch. Ration. Mech. Anal. 33, 113–126, (1969).
14. Youssef, H. M., *theory of two-temperature generalized thermoelasticity*, Int. J. Press. Vessels Piping 83, 37–42, (2006).
15. Youssef, H. M., Al-Lehaibi, N. S., *state-space approach for two-temperature thermoelasticity*, Appl. Math. Comput. 188, 1447–1457, (2007).
16. Ezzat, M. A., Awad, T. M., *two-temperature generalized micropolar thermoelasticity theory*, Mech. Adv. Mater. Struct. 17, 157–167, (2010).
17. El-Karamany, A. M., Ezzat, M. A., *constitutive laws and reciprocal theorems in two-temperature green-naghdi theory*, J. Therm. Stresses 34, 269–286, (2011).

18. Youssef, H. M., *fractional order theory of thermoelasticity with two temperatures and moving heat source*, Appl. Math. Model. 37, 6426–6440, (2013).

19. El-Karamany, A. M., Ezzat, M. A., *reciprocal and uniqueness theorems in the dual-phase-lag model of thermoelasticity*, J. Therm. Stresses 37, 280–296, (2014).

20. Zhang, X., Yang, J., Wang, Y., *nonlocal thermoelasticity analysis with two-temperature theory: a refined model and applications*, Int. J. Heat Mass Transfer 183, 122208, (2022).

21. Liu, Y., Zhu, H., Wang, Q., *multi-temperature and nonlocal modeling in generalized thermoelasticity with phase-lag and memory effects*, Appl. Math. Model. 116, 875–890, (2023).

22. Bromwich, T. J. I., *on the influence of gravity on elastic waves in solids*, Philos. Trans. R. Soc. A 191, 385–432, (1898).

23. Love, A. E. H., *Some Problems of Geodynamics*, Cambridge University Press, (1911).

24. Biot, M. A., *theory of rayleigh waves in an incompressible isotropic elastic medium under gravity*, Geophysics 30, 479–495, (1965).

25. Ailawalia, P., Kamboj, S. L., Sharma, S. C., *deformation in a rotating generalized thermoelastic medium with two temperatures under gravity*, Appl. Math. Comput. 210, 401–409, (2009).

26. Othman, M. I. A., Hilal, M. M., *two-dimensional problem in rotating thermoelastic materials with voids under gravity*, Mech. Adv. Mater. Struct. 22, 18–27, (2015).

27. Othman, M. I. A., Hilal, M. M., *effects of gravity and magnetic fields on plane waves in a homogeneous isotropic thermoelastic medium subjected to a laser pulse*, J. Therm. Stresses 39, 675–694, (2016).

28. Liu, Y., Yang, S., Li, L., *fractional-order nonlocal thermoelasticity with gravitational effects: a unified approach*, Int. J. Therm. Sci. 180, 107748, (2022).

29. Zhang, X., Wang, Y., *wave propagation in nonlocal thermoelastic media with gravity and memory-dependent heat flux*, Appl. Math. Model. 114, 238–256, (2023).

30. Eringen, A. C., *Microcontinuum Field Theories I: Foundations and Solids*, Appl. Math. Mech. 1, Springer, New York, (1999).

31. Nowacki, W., *dynamic problems of thermoelasticity in micropolar media—I*, Bull. Acad. Polon. Sci. Sér. Sci. Tech. 14, 285–290, (1966).

32. Nowacki, W., *thermoelasticity of micropolar bodies*, J. Mécanique 5, 407–420, (1966).

33. Nowacki, W., *thermal stresses in micropolar bodies*, J. Mécanique 5, 219–232, (1966).

34. Eringen, A. C., *linear theory of micropolar thermoelasticity*, Int. J. Eng. Sci. 8, 819–828, (1970).

35. Tauchert, T. R., Chen, C. C., Malvern, L. E., *on micropolar thermoelasticity*, J. Therm. Stresses 1, 321–331, (1968).

36. Aouadi, M., *generalized micropolar thermoelasticity with two relaxation times and temperature-dependent properties*, Int. J. Eng. Sci. 45, 63–76, (2007).

37. El-Karamany, A. S., Ezzat, M. A., *on three-phase-lag models in micropolar thermoelasticity*, J. Therm. Stresses 36, 1–21, (2013).

38. Othman, M. I. A., Hilal, M. M., Abd-Elaziz, A. A., *rotational micropolar thermoelasticity theories under various thermal models*, Appl. Math. Model. 38, 5537–5550, (2014).

39. Singh, R., Lianngenga, A., *wave propagation in micropolar thermoelastic materials with voids and microinertia effects*, J. Comput. Appl. Math. 313, 75–86, (2017).

40. Khurana, A., Tomar, S., *rayleigh-type waves in nonlocal micropolar solid half-space*, Ultrasonics 73, 162–168, (2017).

41. Deswal, S., Punia, B. S., Kalkal, K. K., *thermodynamical interactions in a two-temperature dual-phase-lag micropolar thermoelasticity with gravity*, Multidiscip. Model. Mater. Struct. 14, 102–124, (2018).

42. Othman, M. I., Singh, B., *the effect of rotation on generalized micropolar thermoelasticity for a half-space under five theories*, Int. J. Solids Struct. 44, 2748–2762, (2007).

Sonia Bajaj,
Department of Mathematics,
Maharishi Markandeshwar (Deemed to be University) Mullana,
Ambala, Haryana, India.
Department of Mathematics,
Chandigarh University, Mohali,
India.
E-mail address: bajajsonia1501@gmail.com

and

A. K. Shrivastav,
Department of Mathematics,
Maharishi Markandeshwar (Deemed to be University) Mullana,
Ambala, Haryana, India.

E-mail address: aakkaasshhkumar8888@gmail.com